

A *Spitzer* Survey of Novae in M31

A. W. Shafter¹, M. F. Bode², M. J. Darnley², K. A. Misselt³, M. Rubin¹, and K. Hornoch⁴

ABSTRACT

We report the results of the first infrared survey of novae in the nearby spiral galaxy, M31. Both photometric and spectroscopic observations of a sample of 10 novae (M31N 2006-09c, 2006-10a, 2006-10b, 2006-11a, 2007-07f, 2007-08a, 2007-08d, 2007-10a, 2007-11d, and 2007-11e) were obtained with the *Spitzer* Space Telescope. Eight of the novae were observed with the IRAC (all but M31N 2007-11d and 2007-11e) and eight with the IRS (all but 2007-07f and 2007-08a), resulting in six in common between the two instruments. The observations, which were obtained between ~ 3 and ~ 7 months after discovery, revealed evidence for dust formation in two of the novae: M31N 2006-10a and (possibly) 2007-07f, and [Ne II] $12.8\mu\text{m}$ line emission in a third (2007-11e). The *Spitzer* observations were supplemented with ground-based optical photometric and spectroscopic data that were used to determine the speed classes and spectroscopic types of the novae in our survey. After including data for dust-forming Galactic novae, we show that dust formation timescales are correlated with nova speed class in that dust typically forms earlier in faster novae. We conclude that our failure to detect the signature of dust formation in most of our M31 sample is likely a result of the relatively long delay between nova eruption and our *Spitzer* observations. Indeed, the two novae for which we found evidence of dust formation were the two “slowest” novae in our sample. Finally, as expected, we found that the majority of the novae in our sample belong to the Fe II spectroscopic class, with only one clear example of the He/N class (M31N 2006-10b). Typical of an He/N system, M31N 2006-10b was the fastest nova in our sample, not detected with the IRS, and just barely detected in three of the IRAC bands when it was observed ~ 4 months after eruption.

Subject headings: galaxies: stellar content — galaxies: individual (M31) — stars: novae, cataclysmic variables

¹Department of Astronomy, San Diego State University, San Diego, CA 92182

²Astrophysics Research Institute, Liverpool John Moores University, Birkenhead CH41 1LD, UK

³Steward Observatory, University of Arizona

⁴Astronomical Institute, Academy of Sciences, CZ-251 65 Ondřejov, Czech Republic

1. Introduction

Novae are all semi-detached binary systems where a late-type star transfers mass to a white dwarf companion (Warner 1995, 2008). A thermonuclear runaway eventually ensues in the material accreted onto the surface of the white dwarf resulting in the nova explosion (Starrfield et al. 2008). The resulting release of energy ($\sim 10^{44} - 10^{45}$ ergs) is sufficient to expel the accreted envelope and drive substantial mass loss (10^{-4} – $10^{-5} M_{\odot}$) from the system at high velocities (\sim several hundreds to a few thousand km s^{-1} ; Bode 2010). Novae exhibit outburst amplitudes of roughly 10 to 20 mag, and can reach peak luminosities as high as $M_V \sim -10$, second only to GRB and supernovae in the energetics of their outbursts, but far more frequent in a given galaxy than either. Their high luminosities and rates ($\sim 50 \text{ yr}^{-1}$ in a galaxy like M31 [Shafter & Irby 2001; Darnley et al. 2006]), make novae powerful probes of the properties of binary star systems in different (extragalactic) stellar populations. The rapid formation of copious amounts of dust in many novae post-outburst also makes them unique laboratories in which to explore cosmic dust grain formation (Bode & Evans 1989; Evans & Rawlings 2008; Gehrz 2008).

Models show that properties of the eruption (e.g. the peak luminosity and the decline rate) are strongly dependent on parameters such as the accretion rate, and the mass and luminosity of the white dwarf (e.g., Livio 1992), some or all of which may vary systematically with the underlying stellar population. The strength of the nova outburst is most sensitive to the mass of the accreting white dwarf, with the increased surface gravity of a more massive white dwarf resulting in a higher pressure at the base of the accreted envelope at the time of thermonuclear runaway and a more violent outburst. In addition, since a smaller mass of accreted material is required to achieve the critical temperature and density necessary for a runaway, nova outbursts produced on massive white dwarfs are expected to have shorter recurrence times and faster light curve evolution (Hachisu & Kato 2006). Further, since the mean white dwarf mass in a nova system is expected to decrease as a function of the time elapsed since the formation of the progenitor binary (e.g., Tutukov & Yungelson 1995; Politano 1996) the proportion of fast and bright novae is expected to be higher in a younger stellar population, which should contain on average more massive white dwarfs.

Duerbeck (1990) became the first to formally postulate the existence of two populations of novae: a relatively young population of “disc novae”, which are found in the solar neighborhood and in the LMC, and “bulge novae”, which are concentrated towards the Galactic center and in the bulge of M31, and are characterized by generally slower outburst development. The argument in favor of two nova populations was further developed by Della Valle et al. (1992), who showed that the average scale height above the Galactic plane

for “fast” novae ($t_2 < 13 \text{ d}^1$) is smaller than for novae with slower rates of decline. At about the same time, Williams (1992) was proposing that classical novae could be divided into two classes based on their spectral properties: specifically, the relative strengths of either their Fe II or He and N emission lines. Novae with prominent Fe II lines (“Fe II novae”) usually show P Cygni absorption profiles, tend to evolve more slowly, have lower expansion velocities, and have a lower level of ionization, compared with novae that exhibit strong lines of He and N (“He/N novae”). In addition, the latter novae display very strong neon lines, but not the forbidden lines that are often seen in the Fe II novae. Following up on their earlier work, Della Valle & Livio (1998) noted that Galactic novae with well determined distances that were classified as He/N were concentrated near the Galactic plane, and tended to be faster, and more luminous compared with their Fe II counterparts.

Infrared observations offer another avenue for the study of nova populations. Models for thermonuclear runaways on the surfaces of white dwarfs predict that the ejecta will contain not only accreted gas, but material dredged up from the white dwarf as well. Thus, spectroscopic analysis of the ejecta offers an opportunity to distinguish between eruptions that occur on CO white dwarfs and those occurring on more massive ONe white dwarfs (Gehrz et al. 1998). Eruptions occurring on CO white dwarfs are expected to produce a significant amount of dust, mainly in the form of carbon grains that shroud the central source, and result in warm ($\sim 1000 \text{ K}$) blackbody emission that peaks in the near IR ($\sim 3 \mu\text{m}$) 1 – 4 months after eruption (e.g., Geisel et al. 1970; Ney & Hatfield 1978; Bode & Evans 1982; Gehrz et al. 1995; Gehrz 2008). On the other hand, eruptions seated on the more massive ONe white dwarfs are believed to produce strong forbidden lines of neon ([Ne II] $12.8 \mu\text{m}$ and [Ne VI] $7.6 \mu\text{m}$), but little or no dust. The first observational support for a class of novae occurring on massive ONe white dwarfs was found more than twenty years ago when Gehrz et al. (1985) discovered that the [Ne II] $12.8 \mu\text{m}$ emission line in QU Vul ($\lambda/\Delta\lambda = 67$) reached a flux level ~ 60 times that of the free-free continuum more than four months after eruption. At the time, this was the strongest $12.8 \mu\text{m}$ emission line seen in any astrophysical object. Since that time several additional Galactic novae with an overabundance of Ne have been discovered, and they are collectively referred to as “neon” novae (Gehrz et al. 1985). It appears that up to one-third of novae are of this type, with the remainder being CO novae.

Although much can and has been learned from the study of Galactic novae, the nearby spiral M31, where more than 800 nova candidates have been discovered over the past century (e.g. Pietsch et al. 2007; Shafter 2008, and references therein), offers a unique opportunity to study an equidistant sample of novae from differing stellar environments (bulge and disk)

¹ t_2 is the time in days a nova takes to decline by two magnitudes from maximum light.

while minimizing some of the uncertainties that plague Galactic observations (e.g., highly variable extinction along the lines of sight to different novae). With this motivation in mind, we are currently involved in a multi-wavelength program of photometric and spectroscopic follow-up observations of novae discovered in M31 (Shafter et al. 2010). As a part of this effort focusing on the nature of the white dwarfs (CO vs ONe), we have obtained both IR photometric and spectroscopic observations of a sample of 10 novae in M31 using the IRAC and IRS instruments on board the *Spitzer* Space Telescope. Here, we present the results of our survey.

2. Observations

In order to search for dust formation in a sample of M31 novae we initiated a program of *Spitzer* Infrared Array Camera (IRAC; Fazio et al. 2004) and Infrared Spectrograph (IRS; Houck et al. 2004) observations in early 2007 and 2008. Our observing strategy called for the observations to be triggered approximately three months after discovery of a nova. However, due to the vagaries of *Spitzer* scheduling, our observations were typically executed anywhere from 3 to as long as 7 months after eruption.

During the first year of observations, the same 4 novae were observed with both IRAC and the IRS. The results from the IRS observations were disappointing, with no line emission detected in any nova, and continuous emission detected in just two of the novae. We concluded that most novae had likely faded beyond detectability by the time the IRS observations were scheduled. In order to increase the probability of detection, in the second epoch of observations, we were able to modify our IRS target list to include two more recent novae for observation: M31N 2007-11d and 2007-11e, resulting in line emission being detected in one of these novae. Our *Spitzer* observations are summarized in Table 1.

2.1. IRAC Observations

IRAC data were obtained in all four IRAC bands ($3.6\mu\text{m}$, $4.5\mu\text{m}$, $5.8\mu\text{m}$, $8.0\mu\text{m}$). The IRAC observations consisted of a 12 point Reuleaux dither pattern with a medium scale factor. A single 100 sec frame was obtained at each dither position, resulting in a total of ~ 1200 sec of exposure in each band. Source extraction and photometry were performed on the Post-BCD (Basic Calibrated Data) mosaics produced by the *Spitzer* Science Center (SSC), pipeline version 18.5. The extractions and determination of uncertainties were performed using version 2.1 of the IDL program ATV, written and maintained by Barth (2001).

Due to the crowded nature of the observed fields along with rapidly varying background levels, it was necessary to use apertures of minimal size to avoid contamination from neighboring objects. Therefore we chose an aperture size of radius 2 pixels for each extraction. We used the nominal positions of the novae as determined by visual photometric observations, along with an ATV 3-pixel-radius centering box, to determine the center for each aperture used in extraction. Aperture correction factors, derived by the SSC and provided in the IRAC Data Handbook 3.0, were then used to estimate the true flux of the novae based on the measured flux in each aperture. Finally, we determined the background level for each aperture using an annulus of inner radius of 2 pixels and outer radius 6 pixels. The energy distributions for the six novae detected by IRAC are shown in Figure 1 and summarized in Table 2.

2.2. IRS Observations

IRS data were obtained in the low resolution SL1 module, covering a wavelength range of $7.4 - 14.5\mu\text{m}$. The IRS data were obtained using 24 cycles of 60 sec ramps. As each cycle of an IRS observation consists of two nod positions, this resulted in a total of ~ 2880 sec of on-source integration time per target.

The IRS data were analyzed in the SMART package (Higdon et al. 2004) using optimal extraction (Lebouteiller et al. 2010). The BCD (Basic Calibrated Data) products were cleaned using the IRSCLEAN tool with campaign specific masks before all 2D spectra at a given nod position were combined into a single image. For our observations, this resulted in two ~ 1440 sec cleaned two dimensional spectra. Prior to spectral extraction, the two nod positions were subtracted from each other to remove the background and mitigate rogue pixels not present in the masks. The spectral extraction was performed on these background subtracted images. For each object, we selected the “manual optimal extraction” option in SMART. The position of the IRS slit was projected on our IRAC images to verify that we were extracting spectra for the correct object. A visual inspection of the two dimensional spectra revealed that only 2 objects (M31N 2006-09c and 2006-10a) had clear traces at the nominal source position. For the remaining objects (with the exception of M31N 2007-11e, see below), we extracted spectra at the nominal source position in each nod position. As expected from the visual inspection of the two dimensional spectra, no sources were detected. In the case of M31N 2006-09c, the nova was the only detected source. The spectrum of M31N 2006-09c was extracted using the optimal extraction algorithm with a background order of one; even though background subtraction was accomplished to first order by subtracting nod positions, residual structure was still present owing to the variation of the

local background between the nod positions. In the case of M31N 2006-10a, there were two objects detected, the brighter nova at the nominal position in the slit as well as a fainter source offset by ~ 3 pixels ($\sim 5''$). To extract M31N 2006-10a, two sources were specified and the extraction algorithm was allowed to fit the trace within one pixel of the nominal position (for the nova) and between one and four pixels from the nominal position for the contaminating source. In the case of M31N 2007-11e, no source was apparent save for a faint line at the position of [Ne II] $12.8\mu\text{m}$. For M31N 2007-11e, we forced the extraction aperture to be centered on the nominal source position for each nod. For all three objects, spectra extracted at each nod position were clipped at the order edges and combined. The spectra extracted for M31N 2006-09c and 2006-10a are shown in Figure 2 and the extracted spectrum of M31N 2007-11e is shown in Figure 3.

2.3. Optical Photometric Observations

To complement our *Spitzer* observations, we attempted to obtain optical photometric time-series of several novae in our survey using the Liverpool Telescope (LT, Steele et al. 2004), primarily to measure the peak nova brightness and rate of decline (t_2). The LT data were reduced using a combination of IRAF² and Starlink software. These data were calibrated with standard stars from Landolt (1992) and checked against secondary standards from Magnier et al. (1992), Haiman et al. (1994), and Massey et al. (2006). These observations were augmented by the extensive photometric database compiled by one of us (KH) as part of an on-going program to monitor nova light curves in M31. The latter observations include both survey and targeted images taken with the 0.35-m telescope of private observatory of KH at Lelekovice, the 0.65-m telescope of the Ondřejov observatory (operated partly by the Charles University, Prague), and the 0.28-m telescope of the Zlín observatory. Standard reduction procedures for raw CCD images were applied (bias and dark-frame subtraction and flat-field correction) using SIMS³ and Munipack⁴ programs. Reduced images of the same series were co-added to improve the S/N ratio (total exposure time varied from ten minutes up to about one hour). The gradient of the galaxy background of co-added images was flattened by a spatial median filter using SIMS. These processed images were then used to search for novae. Photometry was performed using “Optimal Photometry” (based on

² IRAF is distributed by the National Optical Astronomy Observatory, which is operated by the Association for Research in Astronomy, Inc. under cooperative agreement with the National Science Foundation.

³<http://ccd.mii.cz/>

⁴<http://munipack.astronomy.cz/>

fitting of PSF profiles) in GAIA⁵, and calibrated with standard stars from Landolt (1992).

Of the ten novae observed by *Spitzer* we were successful in obtaining a series of photometric observations for five of the novae. The results of these observations are summarized in Tables 3 – 7, with the resulting light curves shown in Figures 4 – 6.

2.4. Optical Spectroscopic Observations

In addition to our ground-based photometric observations, we also attempted to obtain optical spectroscopic observations of each nova using the Low Resolution Spectrograph (LRS; Hill et al. 1998) on the Hobby-Eberly Telescope (HET). We used either the *g1* grating with a 1.0'' slit and the GG385 blocking filter covering 4150–11000 Å at a resolution of $R \sim 600$, or the *g2* grating with a 2.0'' slit and the GG385 blocking filter, covering 4275–7250 Å at a resolution of $R \sim 650$. When employing the lower-dispersion *g1* grating, we limited our analysis to the 4150–9000 Å wavelength range where the effects of order overlap are minimal. The spectra were reduced using standard IRAF routines to flat-field the data and to optimally extract the spectra. A summary of all the HET observations is given in Table 8. Because the observations were made under a variety of atmospheric conditions with the stellar image typically overfilling the spectrograph slit, our data are not spectrophotometric. Thus, the data have been displayed on a relative flux scale.

Spectra were successfully obtained for eight of the ten novae observed by *Spitzer*. These data, which were obtained primarily to ascertain the spectroscopic classes (Williams 1992) and ejection velocities of the novae, are shown in Figures 7 – 9, and are summarized in Tables 9 and 10. Spectroscopic classes for the two novae that we were unable to observe, M31N 2007-07f and 2007-08a, were available through spectra obtained by Quimby (2007) and Barsukova et al. (2007), respectively.

Seven of the ten novae in our sample clearly belong to the Fe II class, which is characterized by relatively narrow Balmer and Fe II emission. Of the remaining three, M31N 2006-10b was a “hybrid” nova (a broad-lined Fe II system that later evolved into a He/N system), while M31N 2007-08a was described by Barsukova et al. (2007) as an Fe II (or possibly a hybrid) nova. The large Balmer emission line widths seen in M31N 2006-10b are typical of what is found in He/N novae; however, the relatively narrow lines exhibited by 2007-08a are more characteristic of the Fe II class. The remaining nova, M31N 2007-10a, is quite peculiar spectroscopically (see Figure 8). The spectrum displays narrow emission characteristic of

⁵<http://www.starlink.rl.ac.uk/gaia>

the Fe II novae, but in addition to Balmer emission, shows prominent He I lines rather than Fe II emission.

The spatial positions of the 10 novae in our *Spitzer* sample are shown in Figure 10. As has been demonstrated by Shafter (2007) from a larger sample of novae, there is no evidence that the spatial distribution of Fe II and He/N novae differ in M31 (see also Shafter et al. 2010).

3. Discussion

Of the 8 novae observed by IRAC, only M31N 2006-10a shows clear evidence of an infrared excess in the IRAC bands, peaking at $\lambda \sim 4\mu\text{m}$ (see Fig. 2). M31N 2007-07f shows evidence for a rather weaker, slightly longer wavelength excess (see Fig. 1). We may associate such excess emission with that from dust grains condensing in the ejecta of each nova, as has been observed in many Galactic novae – see Section 1. Both M31N 2006-10a and 2007-07f belong to the Fe II spectroscopic class, and both can be considered relatively “slow” novae with decay times of $t_2(V) = 83$ and $t_2(R) \sim 50$ days, respectively.

To further explore the relationship between dust formation timescales and nova speed class, we have augmented our M31 sample with available data on Galactic dust-forming novae. A summary is presented in Table 11. In Figure 11 we have plotted the condensation time, t_{cond} , of dust grains in Galactic novae against t_2 . Dust condensation times for this plot have been taken from Table 13.1 of Evans & Rawlings (2008) and times of dust breaks in D-type novae from Strophe et al. (2010). In general, these are consistent within a few days, but we have taken the earlier quoted time in each case, if they are both available for a given nova. Speed class, in terms of t_2 , has been taken from Strophe et al. (2010). We have also plotted the two suspected dusty M31 novae on Figure 11, where t_{cond} is likely to be an upper limit in both instances (i.e. we have not necessarily observed the onset of the dust formation event). Note that for M31N 2006-10a and 2007-11d, we have used $t_2(V)$ but as this was unavailable for the other M31 novae, we have used $t_2(R)$.

There is a clear trend for the Galactic novae in the sense that the faster novae tend to form grains earlier than the slow novae. An outlier is nova PW Vul. Gehrz et al. (1988) note that this nova had a very erratic early optical light curve which resembled DQ Her, but showed no deep minimum as did the latter, archetypal dust-forming nova. Indeed PW Vul’s dust shell was also low mass and optically thin and the quoted value of $t_{\text{cond}} = 154$ days was calculated by Gehrz et al. (1988) from the angular expansion rate of the pseudo-photosphere and the maximum flux of the outburst. This is consistent with the time of

first condensation being in the observational gap between 100 and 290 days post-outburst. Also shown as a lower limit on this plot is the dust condensation time for QU Vul, given by Evans & Rawlings (2008) as 40–200 days (we will return to this object below). Marking an extreme point on the plot is nova V445 Pup. A dust extinction dip is clearly seen in its light curve and (relatively sparse) infrared photometry thereafter confirms the presence of an extensive dust shell, but this is an example of a very rare Helium nova outburst (see Woudt et al. 2009, and references therein).

The apparent correlation between t_{cond} and t_2 is perhaps surprising. If we assume a constant central source luminosity, L_* , and outflow velocity, v_{ej} , for a given nova, and that the grain condensation temperature, T_{cond} , is constant from nova to nova, we can write (e.g., Gehrz 2008):

$$t_{\text{cond}} \propto L_*^{0.5} v_{\text{ej}}^{-1}. \quad (1)$$

Adopting available empirical relations between v_{ej} and t_2 , and between L_* and t_2 (the Maximum-Magnitude vs Rate-of-Divide relation) such as those given in Warner (2008), we find that $v_{\text{ej}} \propto t_2^{-0.5}$ and $L \propto t_2^{-1}$. After inserting these relations into eqn (1), it appears that t_{cond} should be essentially independent of nova speed class! Clearly, the empirical correlation shown in Figure 11 justifies further investigation, but as pointed out by Evans & Rawlings (2008), dust grain nucleation and growth rely on a complex set of parameters. Finally, it should be noted that not all novae form detectable amounts of dust, with examples at both ends of the range of speed class (e.g. V1500 Cyg versus HR Del; Bode & Evans 1989). The reasons for this have been explored by various authors (e.g., Gallagher 1977; Bode & Evans 1983) but are not fully understood.

Figure 12 shows a plot of nova speed class versus the time of maximum infrared flux, t_{IRmax} , as observed in Galactic novae. Since t_{IRmax} is not available for our M31 novae, we have instead plotted the speed class and time after discovery (approximate optical maximum) for the novae observed with IRAC. Both M31N 2006-10a and 2007-07f are marked on the plot. Again there appears to be a trend of increasing t_{IRmax} with speed class for the Galactic novae, with the exception of QU Vul. We may note however that this is the time of the maximum flux observed in the $10\mu\text{m}$ silicate feature in this nova by Gehrz et al. (1986) at $t = 240$ days, and not necessarily the time of maximum continuum emission from grains in the expanding shell, which may have been (much) earlier. Indeed, an observation on day 206 for this nova by Smith et al. (1995) showed that at this time emission from graphitic dust clearly dominated the $10\mu\text{m}$ continuum in QU Vul.

From Figure 12, it appears that M31N 2006-10a may have been observed by *Spitzer*

nearer the time of the infrared emission maximum than 2007-07f, which again is consistent with the higher dust shell luminosity and inferred dust temperature in 2006-10a compared to 2007-07f. Indeed, M31 2006-10a might have been observed not too long after t_{cond} at around the time of t_{IRmax} . Evidence for this comes from its position on Figs. 11 and 12, coupled with T_{BB} ($\sim 720 \pm 100\text{K}$) being much lower than T_{cond} ($\sim 1200\text{K}$). There is in fact a steep drop in observed effective dust grain temperature in well observed dusty novae coinciding approximately with infrared maximum arising from what Bode & Evans (1983) termed the “infrared pseudo-photosphere” in the optically thick (in the infrared) dust shells of prolific dust formers such as NQ Vul (Ney & Hatfield 1978). As the dust formation rate reduces in the expanding shell, the observed optical depth also reduces and T_{BB} increases again. Mitchell et al. (1983) found even better agreement with observations if grains were subject to some size reduction around the time of infrared maximum, possibly due to sputtering. In NQ Vul the temperature minimum lasted from around 62 to 130 days post-outburst.

All but one of the faster M31 novae lie above the region occupied by the Galactic novae at infrared maximum (the exception being M31N 2006-11a). The non-detection of dust emission in these objects may then be due to them either being observed well after dust emission maximum, or the fact that they did not produce large amounts of dust in the first place. The latter appears to be the case for 2006-11a at least, as it does lie in the region of the plot occupied by the dusty Galactic novae.

We may estimate the total mass of dust in M31N 2006-10a, M_{d} , assuming an isothermal, optically-thin dust shell of uniform spherical grains of radius a from the equation

$$M_{\text{d}} \approx a \rho_{\text{g}} d^2 F_{\lambda} \frac{B(\lambda, T_{\text{g}})}{Q_{\text{abs}}(\lambda, a)}, \quad (2)$$

where d is the distance, ρ_{g} the bulk density of the grain material, F_{λ} the observed flux density at wavelength λ , B the Planck function at λ and grain temperature T_{g} , and Q_{abs} the grain absorption coefficient. If $Q_{\text{abs}} \propto \lambda^{-\alpha}$ for small dielectric absorbers, it can be shown that

$$T_{\text{g}} = \frac{2890}{\lambda_{\text{max}}} \left(\frac{5}{\alpha + 5} \right), \quad (3)$$

where λ_{max} is the wavelength of maximum emission in μm .

In the case of M31N 2006-10a, the IRS spectrum in Figure 2 shows no apparent $10\mu\text{m}$ silicate feature, and the emitting grains are more likely carbon-based, as seen at some point in the evolution of most dust-forming novae (Evans & Rawlings 2008; Gehrz 2008). Taking for simplicity graphite spheres of size small compared with the wavelength of emission, then

$\alpha \approx 2$ (Evans 1994). Thus with $\lambda_{\max} = 4\mu\text{m}$, $T_g = 516$ K, and if $a = 0.1\mu\text{m}$, then $Q_{\text{abs}} = 4.72 \times 10^{-2}$ (Draine 1985, although this neglects any temperature dependence of the absorption coefficient). Taking $\rho_g = 2000$ kg m $^{-3}$ (Love et al. 1992), and a distance to M31 of 780 kpc (Holland 1998; Stanek & Garnavich 1998) then $M_d \sim 2 \times 10^{-6} M_{\odot}$. This is consistent with the range of dust masses derived for Galactic novae, particularly the more prolific dust-formers (see e.g., Gehrz 2008).

4. Summary and Conclusions

We have conducted the first infrared survey of novae in the nearby spiral, M31, using the *Spitzer* Space Telescope. The primary motivation behind the survey was to determine the feasibility of using *Spitzer* observations of M31 novae to study dust formation property as a function of nova speed class and spectroscopic type. We observed a total of 10 novae in M31 with *Spitzer* over a two year period: M31N 2006-09c, 2006-10a, 2006-10b, 2006-11a, 2007-07f, 2007-08a, 2007-08d, 2007-10a, 2007-11d, and 2007-11e. Eight of these novae were observed with IRAC (all but M31N 2007-11d and 2007-11e) and 8 with the IRS (all but M31N 2007-07f and 2007-08a), with 6 novae observed with both instruments.

Observations of Galactic novae show that dust formation typically occurs with a timescale, t_{cond} , of between ~ 1 and ~ 5 months post-eruption (mean ~ 2 months), depending on the speed class of the nova. For a typical nova, the peak infrared signature occurs shortly thereafter, with the time to infrared maximum, t_{IRmax} , averaging about 3 months post-eruption. Thus, our observing strategy was to schedule our *Spitzer* observations approximately 3 months post discovery when the infrared signature due to dust formation was expected to reach a maximum. Unfortunately, the constraints imposed by the *Spitzer* scheduling process did not allow us to time our observations as precisely as we would have liked, and our observations occurred anywhere between ~ 3 and ~ 7 months post eruption. Our principal conclusions can be summarized as follows:

(1) We were able to detect six of the eight novae observed with IRAC. Of these, only M31N 2006-10a showed clear evidence for an infrared excess peaking at $\lambda \sim 4\mu\text{m}$. The IRS spectrum of this nova showed no evidence of silicate emission features and thus we assume that the dust was carbon-based in this case. We were then able to estimate the total mass of dust formed to be $M_d \sim 2 \times 10^{-6} M_{\odot}$. This is comparable to the mass of dust found in Galactic novae forming the more extensive dust shells. Another nova, M31N 2007-07f, showed evidence of possible dust formation through a weaker infrared excess detected to peak at longer wavelength. Our observations of these two novae occurred 116 and 203 days post discovery, respectively. Thus, it is plausible that that our observations of M31N 2007-

07f occurred after the peak IR flux was achieved as suggested by our comparison with the times of infrared maximum in Galactic dust-forming novae. Both novae are Fe II systems with relatively slow light curve evolution: $t_2(V) = 82$ d and $t_2(R) \sim 50$ d, respectively.

(2) We find a surprising correlation between the condensation time for dust grains (t_{cond}) and nova speed class (t_2) for Galactic novae (see Fig. 11). Although upper limits, the values of t_{cond} for the two M31 novae with detected IR excesses are consistent with this correlation. Most of the M31 novae in our sample, which have $t_2 < \sim 50$, were likely observed too long after dust condensation for us to detect an IR excess in our data. One exception is M31N 2006-11a, which is a moderate-speed-class, Fe II nova observed less than 3 months after discovery. A comparison with Galactic dust-forming novae (see Fig 12) shows that an IR excess likely would have been visible assuming dust formation had taken place.

(3) Three of the eight novae observed with the IRS were detected: M31N 2006 09c and 2006-10a showed only continuum emission, while 2007-11e revealed a [Ne II] $12.8\mu\text{m}$ emission feature characteristic of the class of “Neon Novae”. Other than its neon emission, M31N 2007-11e, is fairly unremarkable in other respects, being neither a particularly fast or slow Fe II system.

Our preliminary survey has demonstrated that IR observations can be used to detect dust formation in M31 novae. It is likely that those novae that went undetected were observed too long after maximum light when the dust had cooled sufficiently to render the IR flux below our limit of detection. Future observations, possibly from the ground, of a larger sample of novae will be required to further characterize the relationship between nova speed class, spectroscopic type, and dust formation timescales. The correlations we find between speed class and t_{cond} and t_{IRmax} will greatly assist observational planning.

The work presented here is based in part on observations obtained with the Hobby-Eberly Telescope, which is operated by McDonald Observatory on behalf of the University of Texas at Austin, the Pennsylvania State University, Stanford University, the Ludwig-Maximilians-Universitaet, Munich, and the George-August-Universitaet, Goettingen. Public Access time is available on the Hobby - Eberly Telescope through an agreement with the National Science Foundation. The Liverpool Telescope is operated on the island of La Palma by Liverpool John Moores University in the Spanish Observatorio del Roque de los Muchachos of the Instituto de Astrofisica de Canarias with financial support from the UK Science and Technology Facilities Council (STFC). KH is grateful for obtaining and providing of M31 images to P. Kušnirák, M. Wolf, P. Zasche, P. Cagaš, and T. Henych. AWS is grateful to the NSF for support through grant AST-0607682, and to the University of Victoria for hospitality during his sabbatical leave while this work was being completed.

REFERENCES

- Barth, A. J. 2001, in ASP Conf. Ser., Vol. 238, *Astronomical Data Analysis Software and Systems X*, eds. F. R. Harnden, Jr., F. A. Primini, & H. E. Payne (San Francisco: ASP), 385
- Barsukova, E., Borisov, N., Fabrika, S., Sholukhova, O., Valeev, A., Goranskij, V., Burwitz, V., Pietsch, W.; Hatzidimitriou, D. 2007, *ATel*, 1186, 1
- Bode, M. F. 2010, *AN*, 331, 160
- Bode, M. F., & Evans, A. 1982, *MNRAS*, 200, 175
- Bode, M. F., & Evans, A. 1983, *MNRAS*, 203, 285
- Bode, M. F., & Evans, A. 1989, in *Classical Novae*, 1st Ed., edited by M.F. Bode and A. Evans, J. Wiley, Chichester, p163
- Darnley, M. J. et al. 2006, *MNRAS*, 369, 257
- Della Valle, M., Bianchini, A., Livio, M., & Orio, M. 1992, *A&A*, 266, 232
- Della Valle, M., & Livio, M. 1998, *ApJ*, 506, 818
- Di Mille, F., Ciroi, S., Rafanelli, P., Navasardyan, H., & Bufano, F. 2007, *ATel* 1325.
- Duerbeck, H. W. 1990, in *Physics of Classical Novae*, ed. A.Cassatella & R. Viotti, (New York: Springer-Verlag), 96
- Draine, B.T. 1985, *ApJS*, 57, 587
- Evans, A 1994, *The Dusty Universe*, J. Wiley, Chichester
- Evans, A, & Rawlings, J.M.C. 2008, in *Classical Novae*, 2nd Ed., edited by M.F. Bode and A. Evans, Cambridge University Press, p308
- Fazio, G. G., et al. 2004, *ApJS*, 154, 10
- Gallagher, J. S. 1977, *AJ*, 82, 209
- Gal-Yam, A. & Quimby, R. 2007, *ATel*, 1236
- Gehrz, R. D., Grasdalen, G. L. Hackwell, J. A. 1985, *ApJ*, 298, L47
- Gehrz, R. D., Grasdalen, G. L., Greenhouse, M., Hackwell, J. A., Hayward, T., & Bentley, A. F. 1986, *ApJ*, 308, L63

- Gehrz, R. D., Jones, T. J., Matthews, K., Neugebauer, G., Woodward, C. E., Hayward, T. L., Greenhouse, M. A. 1995, AJ, 110, 325
- Gehrz, R.D., Harrison, T.E., Ney, E.P., Matthews, K., Neugebauer, G., Elias, J., Grasdalen, G.L., & Hackwell, J.A. 1988, ApJ, 329, 894
- Gehrz, R.D., Truran, J. W., Williams, R. E., Starrfield, S. 1998, PASP, 110, 3
- Gehrz, R.D. 2008, in *Classical Novae*, 2nd Ed., edited by M.F. Bode and A. Evans, Cambridge University Press, p167
- Geisel, S. L., Kleinmann, D. E., Low, F. J 1970, ApJ, 161, L101
- Hachisu, I. & Kato, M. 2006, ApJS, 167, 59
- Haiman et al., 1994, A&A, 286, 725
- Higdon, S. J. U., Devost, D., Higdon, J. L., Brandl, B. R., Houck, J. R., Hall, P., Barry, D., Charmandaris, V, Smith, J. D. T., Sloan, G. C.m & Green, J. 2004, PASP, 116, 975
- Hill, G. J., Nicklas, H. E., MacQueen, P. J., Tejada, C., Cobos Duenas, F. J., & Mitsch, W. 1998, Proc. SPIE, 3355, 375
- Holland, S. 1998, AJ, 115, 1916
- Houck et al. 2004, ApJS 154, 18
- Landolt, 1992, AJ, 104, 340
- Magnier et al.,1992, A&AS, 96, 379
- Massey et al., 2006, AJ, 131, 2478
- Livio, M. 1992, ApJ, 393, 516
- Love, S. G., Joswiak, D. J., & Brownlee, D. E. 1992, Icarus, 111, 227
- Mitchell, R. M., Evans, A., & Bode, M. F. 1983, MNRAS, 205, 1141
- Ney, E. P., & Hatfield, B. F. 1978, ApJ, 219, L111
- Lebouteiller, V., Bernard-Salas, J., Sloan, G. C., & Barray, D. J. 2010, PASP, 122, 231
- Pietsch, W., Haberl, F., Sala, G., Stiele, H., Hornoch, K., Riffeser, A., Fliri, J., Bender, R., Bhlér, S., Burwitz, V., Greiner, J. & Seitz, S. 2007, A&A, 465, 375

- Politano, M. 1996, ApJ, 465, 338
- Quimby, R. 2007, ATel, 1161
- Quimby, R., Shafter, A., Rau, A., Kasliwal, M., Ofek, E., Yuan, F., Akerlof, C., Wheeler, J. C., ATel, 1299
- Shafter, A. W. & Irby, B. K. 2001, ApJ, 563, 749
- Shafter, A. W., Coelho, E. A., Misselt, K. A., Bode, M. F., Darnley, M. J., Quimby, R. 2006, ATel, 923
- Shafter, A. W. 2007, presented at “Paths to Exploding Stars: Accretion and Eruption”, Mar 21, 2007, Kavli Institute for Theoretical Physics, UCSB.
- Shafter, A. W. 2008, in *Classical Novae*, 2nd ed., edited by M. Bode and A. Evans, Cambridge University press, p. 335.
- Shafter, A. W., Rau, A., Quimby, R. M., Kasliwal, M. M., Bode, M. F., Darnley, M. J., & Misselt, K. A. 2009, ApJ, 690, 1148
- Shafter, A. W., Darnley, M. J., Bode, M. F., Misselt, K. A., Filippenko, A., Hornoch, K. 2010, ApJS, in preparation.
- Smith, C. H., Aitken, D. K., Roche, P. F., & Wright, C. M. 1995, MNRAS, 277, 259
- Stanek, K.Z., & Garnavich, P.M. 1998, ApJ, 503, L131
- Strope, R.J., Schaefer, B.E., & Henden, A.A. 2010, AJ, 140,34
- Starrfield, S., Iliadis, C., & Hix, R. 2008, in *Classical Novae*, 2nd ed., edited by M. Bode and A. Evans, Cambridge University Press, p. 77.
- Steele I. A., et al., 2004, SPIE, 5489, 679
- Tutukov, A. V. & Yungelson, L. R. 1995, *Cataclysmic Variables*, Proceedings of the conference held in Abano Terme, Italy, 20-24 June 1994 Publisher: Dordrecht Kluwer Academic Publisher:s, 1995. Edited by A. Bianchini, M. della Valle, and M. Orio. *Astrophysics and Space Science Library*, Vol. 205, p.495.
- Warner, B. 1995, in *Cataclysmic Variable Stars*, Cambridge University Press.
- Warner, B. 2008, in *Classical Novae*, 2nd ed., edited by M. Bode and A. Evans, Cambridge University Press, p. 16

Williams, R. E. 1992, AJ, 104, 725

Woudt, P. A., et al. 2009, ApJ, 706, 738

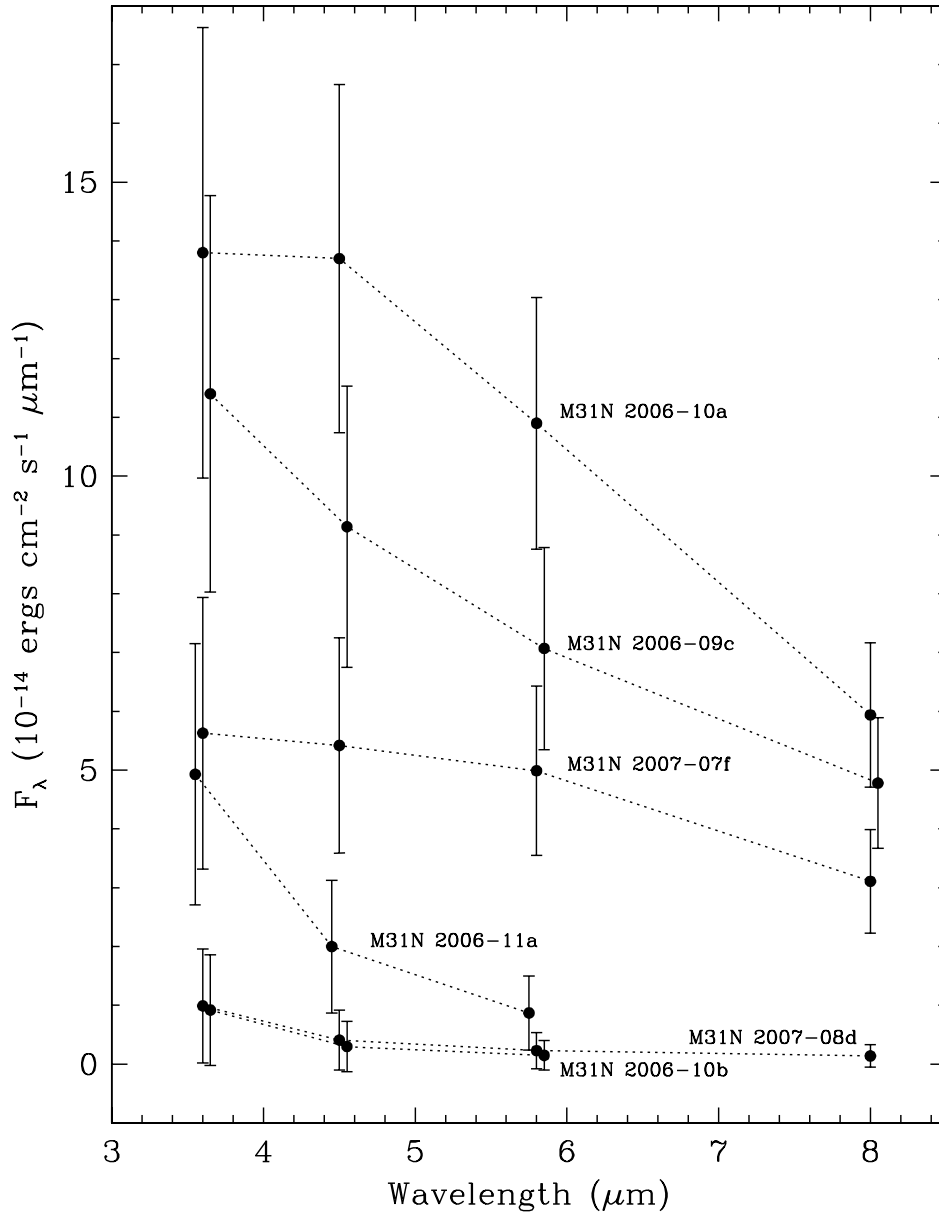


Fig. 1.— The near infrared energy distributions for the six M31 novae detected by our *Spitzer* IRAC observations. The data for M31N 2006-09c, 2006-11a, and 2006-10b have been offset slightly in wavelength for clarity. Note the apparent IR excess in M31N 2006-10a and possibly in 2007-07f.

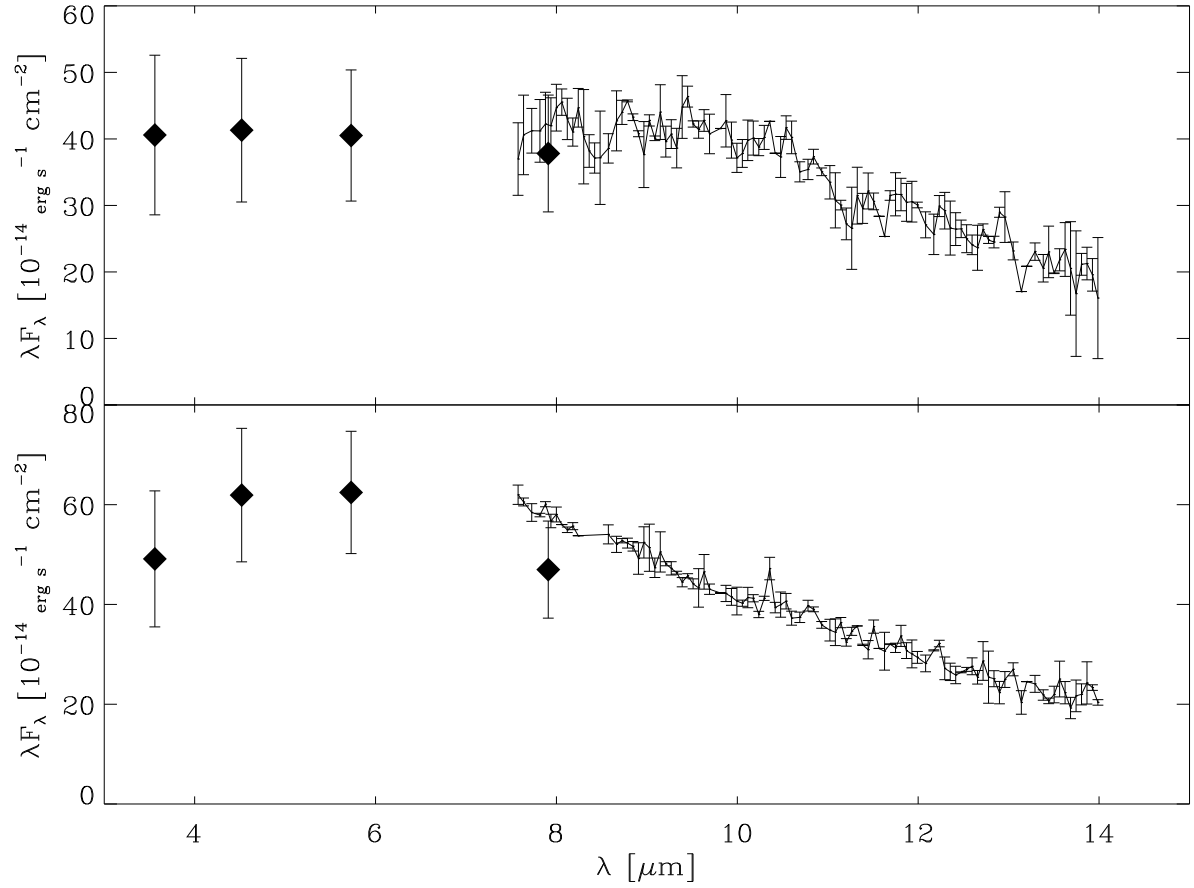


Fig. 2.— The infrared spectral energy distributions for the two novae detected by both IRAC and the IRS: M31N 2006-09c (upper panel) and 2006-10a (lower panel). The IR excess, peaking in λF_λ at $\lambda \sim 5\mu\text{m}$, is obvious in M31N 2006-10a.

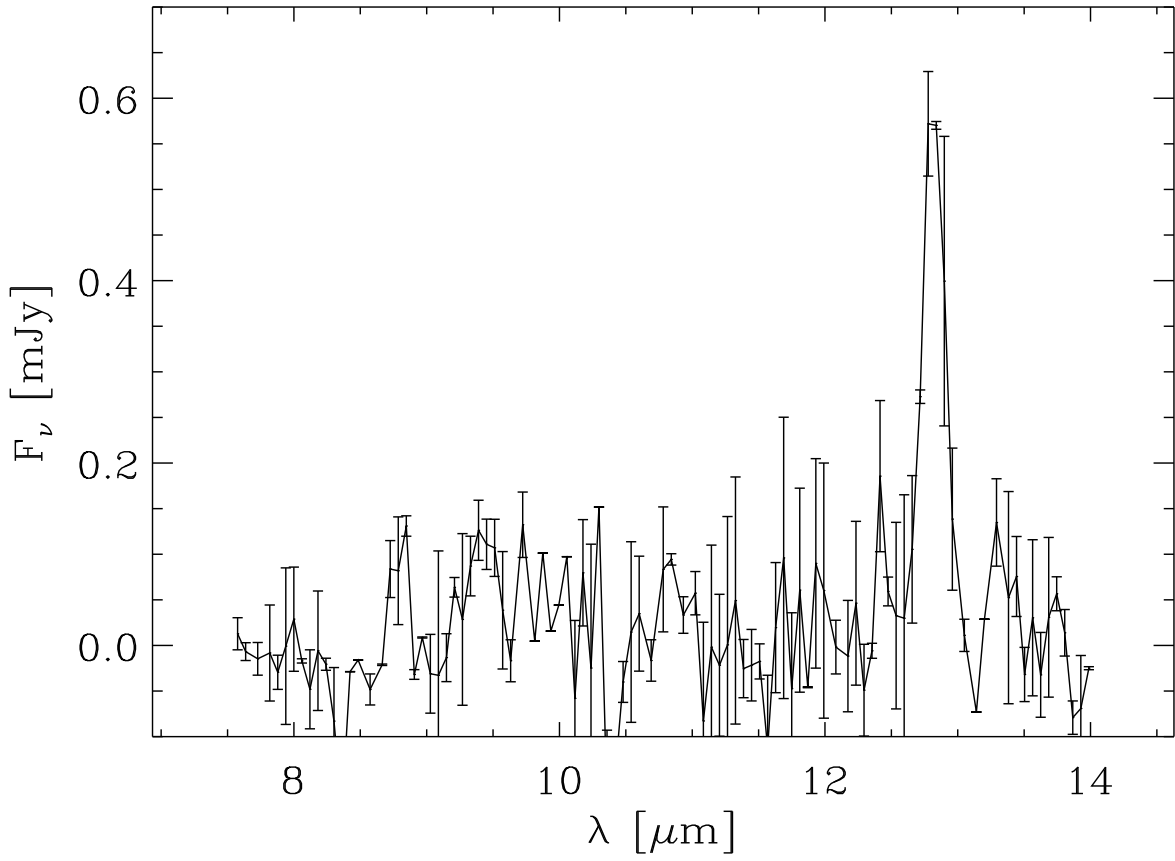


Fig. 3.— The IRS spectrum of M31N 2007-11e showing the [Ne II] $12.8\mu\text{m}$ line in emission, characteristic of the so-called “neon novae”.

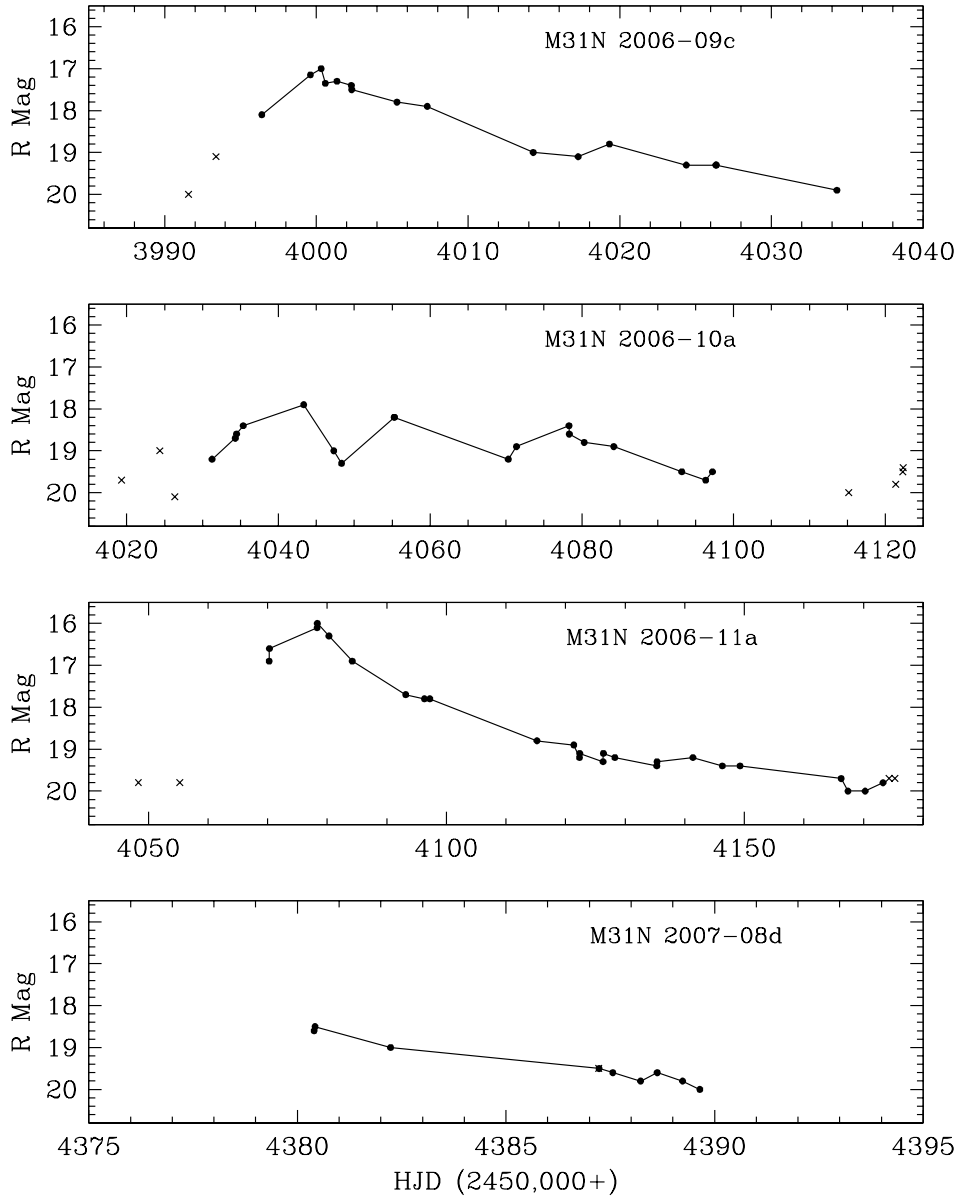


Fig. 4.— R -band light curves for four novae observed by *Spitzer*. The \times symbols refer to lower limits on the R magnitudes. The light curves yield $t_2(R) = 17$ d, $t_2(R) = 112$ d, $t_2(R) = 21$ d, and $t_2(R) = 14$ d for M31N 2006-09c, 2006-10a, 2006-10b, and 2007-08d, respectively.

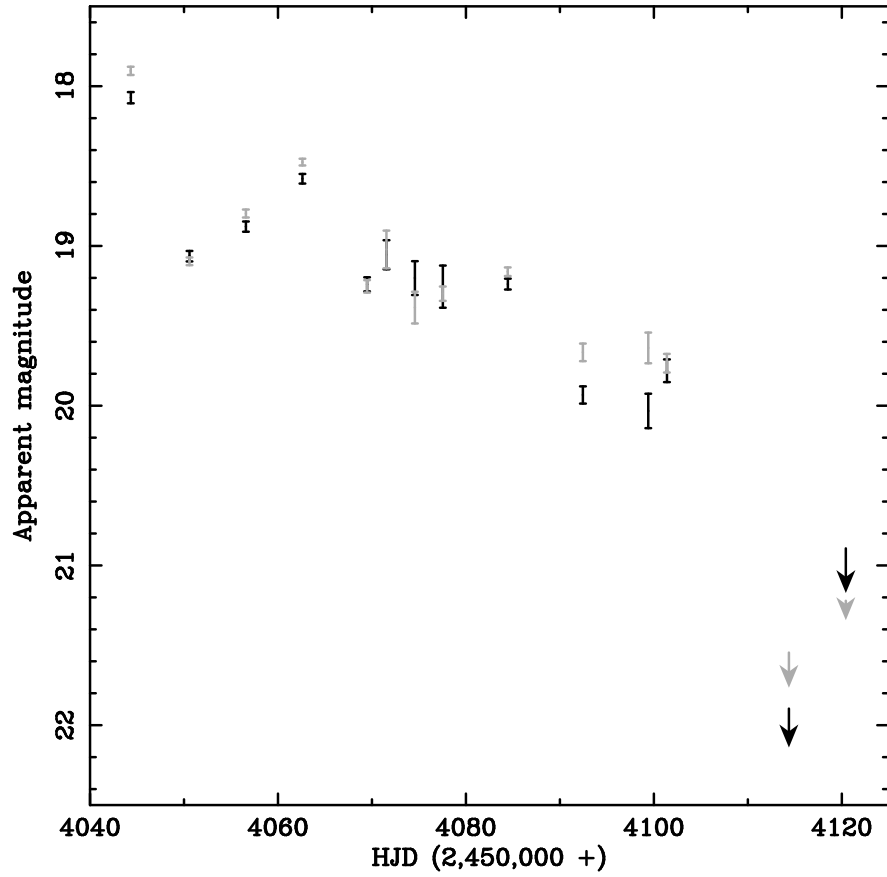


Fig. 5.— The B and V light curves for M31N 2006-10a obtained with the Liverpool Telescope (The V light curve is shown in grey). Arrows are upper limits. From these light curves we derive $t_2(B) = 74$ d and $t_2(V) = 83$ d.

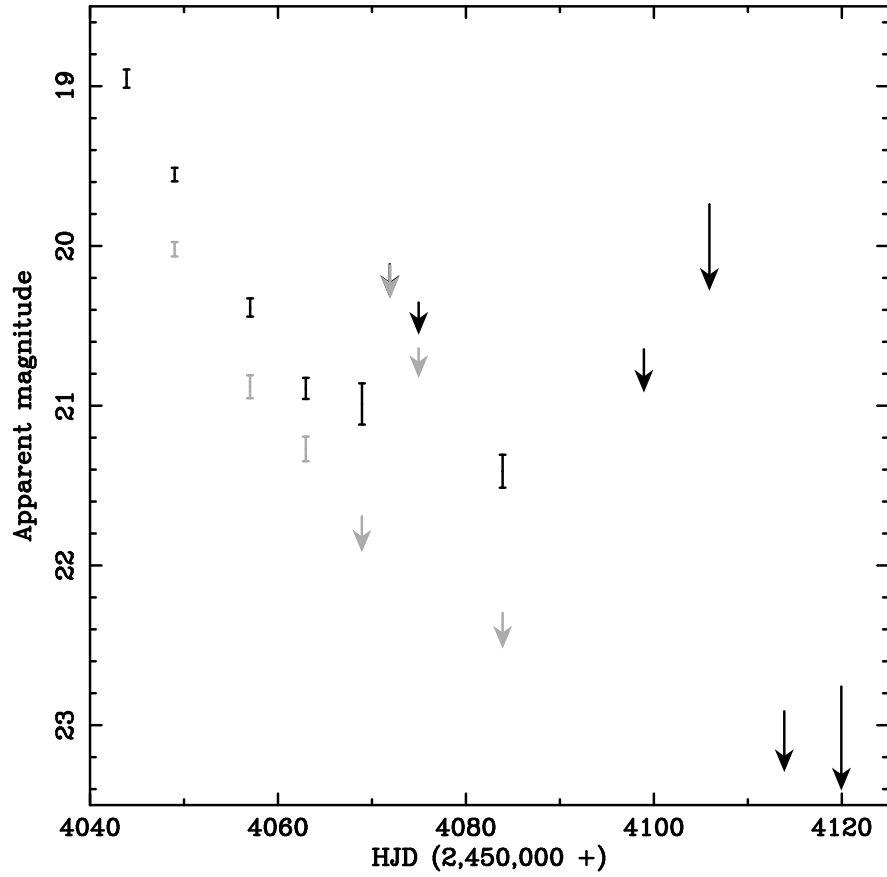


Fig. 6.— The B and V light curves for M31N 2006-10b obtained with the Liverpool Telescope (The V light curve is shown in grey). Arrows are upper limits. Maximum light was missed in V , but the B light curve yields $t_2(B) = 20$ d.

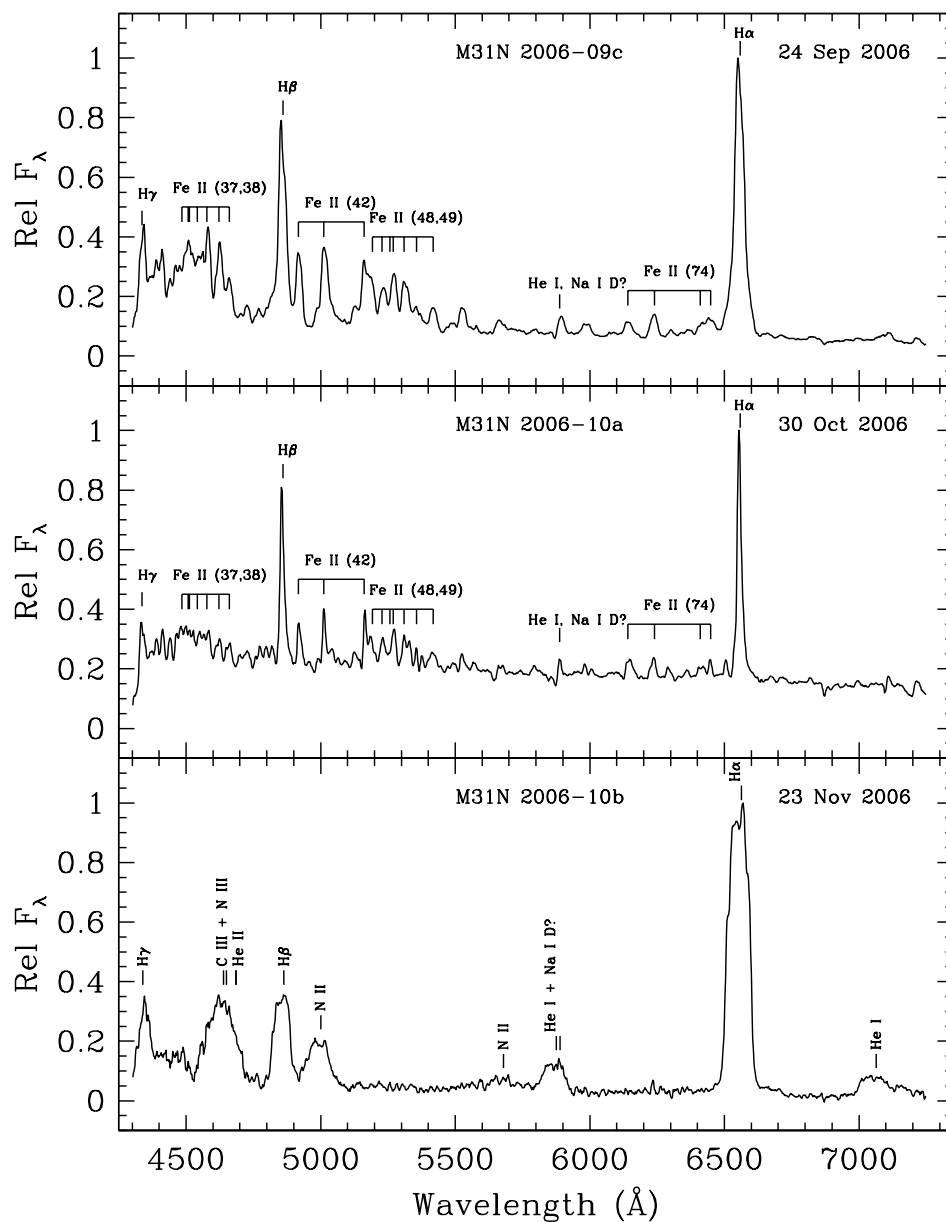


Fig. 7.— HET Spectra of M31N 2006-09c, 2006-10a, and 2006-10b. Note the broad Balmer, He, and N emission lines in M31N 2006-10b characteristic of the He/N spectroscopic class.

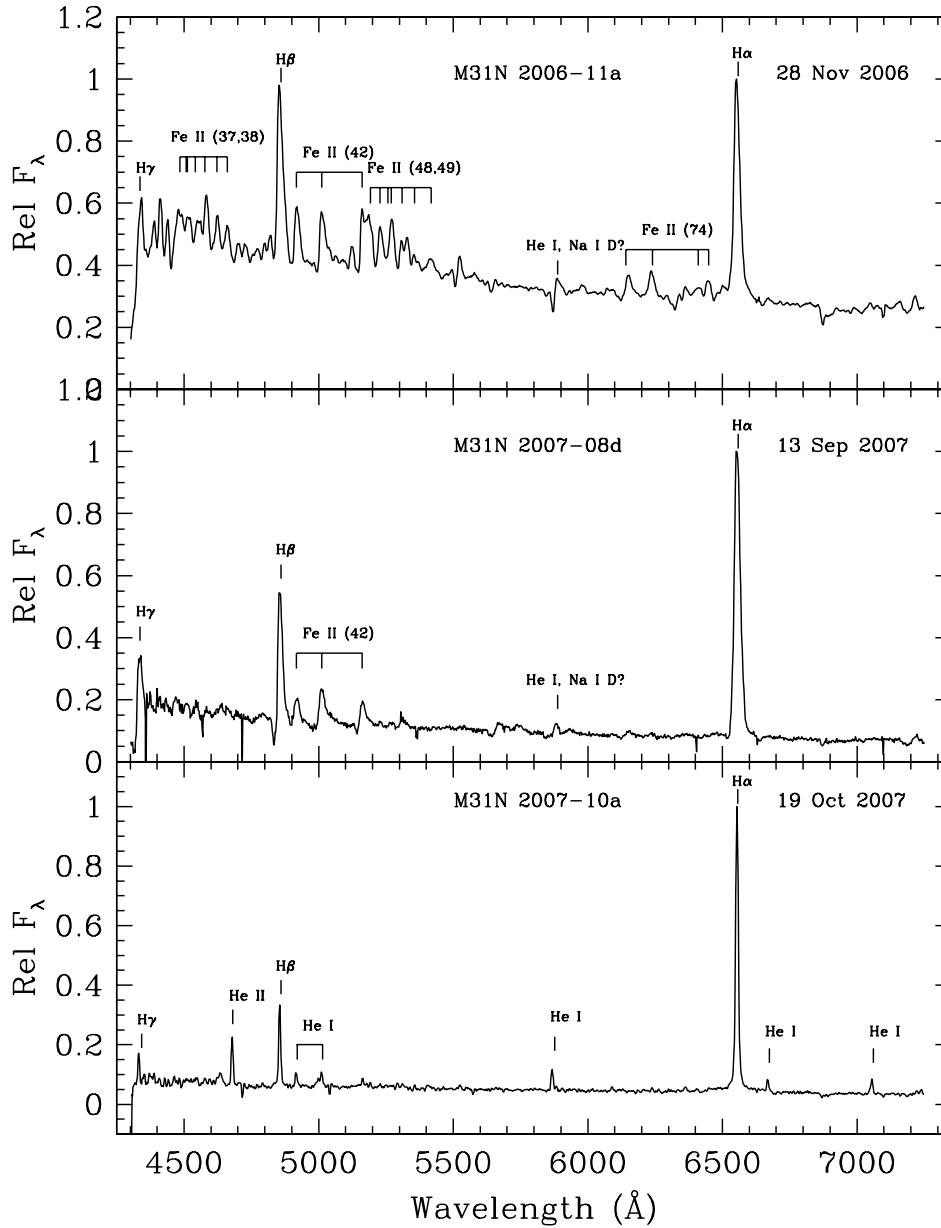


Fig. 8.— HET Spectra of M31N 2006-11a, 2007-08d, and 2007-10a. The spectrum of the latter nova is peculiar in that it has characteristics of both the Fe II and He/N classes (narrow Balmer and He I emission lines without significant Fe II emission).

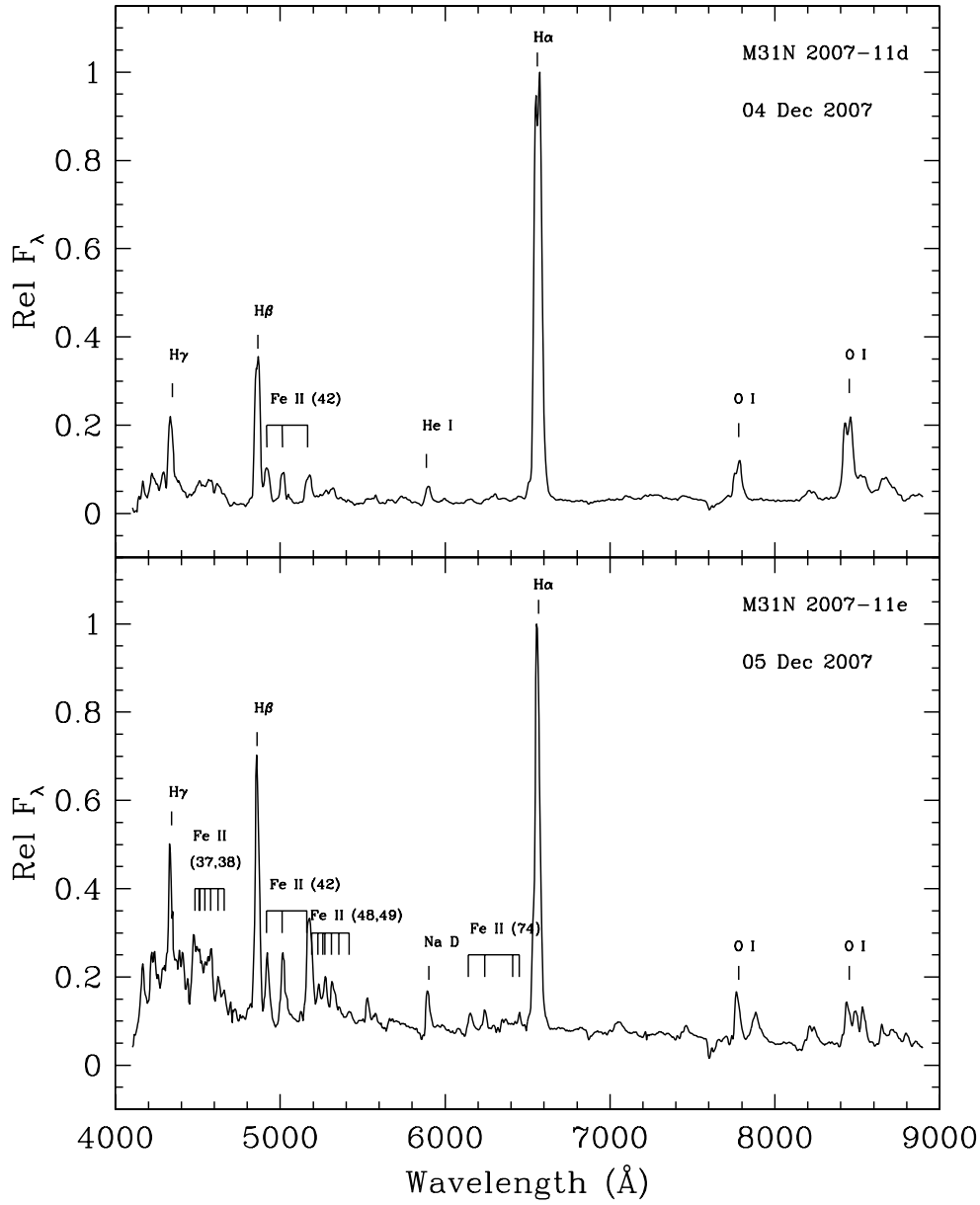


Fig. 9.— HET Spectra of M31N 2007-11d and 2007-11e. Both novae are typical Fe II systems.

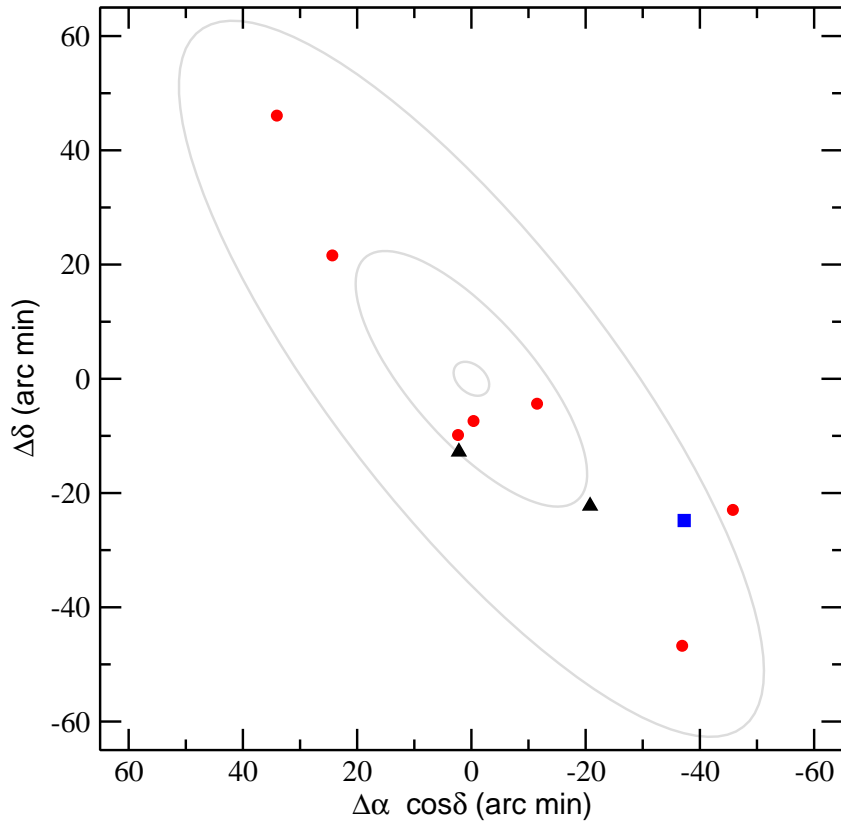


Fig. 10.— The spatial distribution of the 10 M31 novae observed with *Spitzer*. The Fe II novae are indicated by red circles, M31N 2006-10b, the Hybrid nova that evolved into a He/N nova is indicated by a blue square, and the two novae (M31N 2007-08a and 2007-10a) of uncertain type by black triangles.

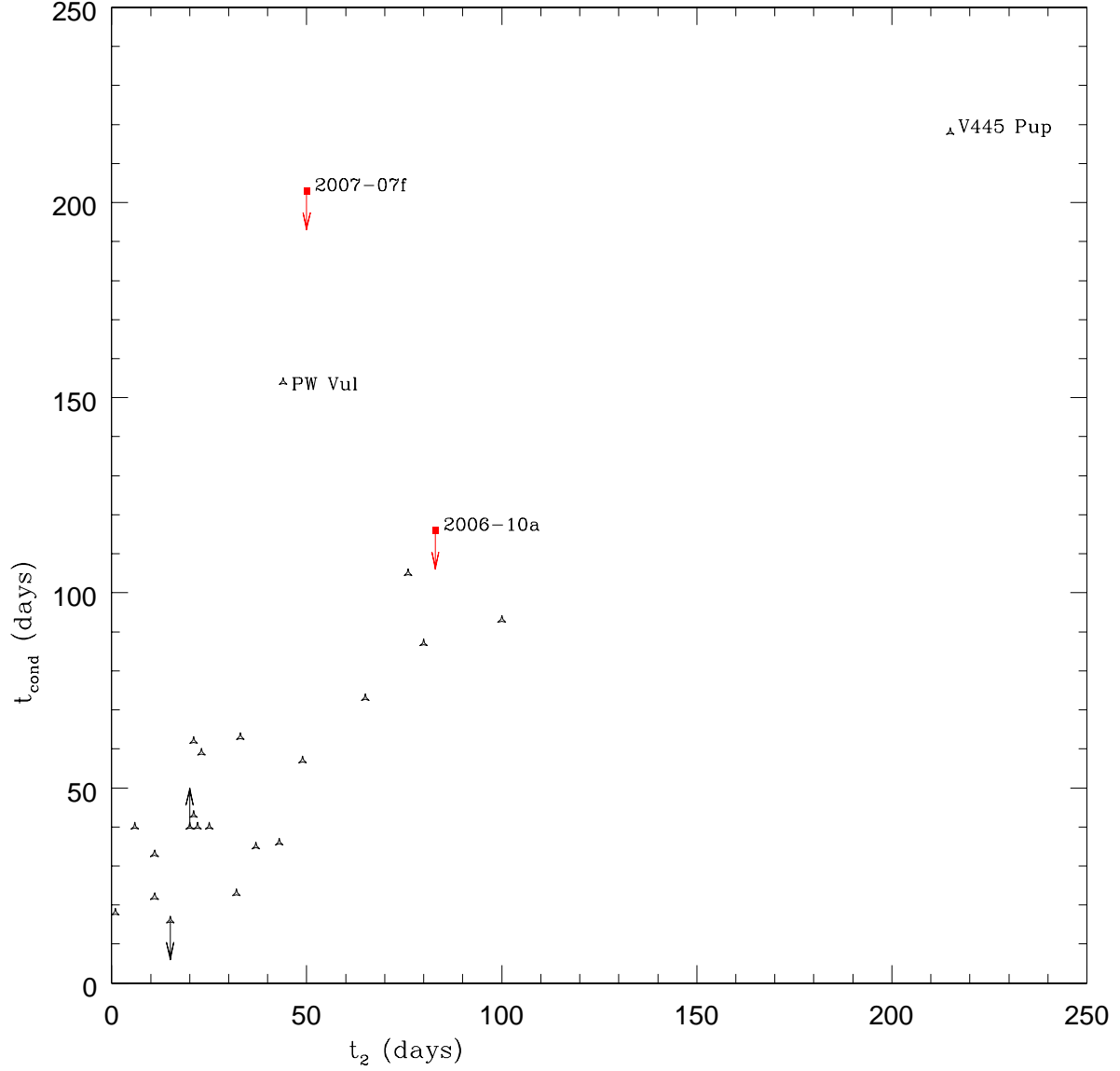


Fig. 11.— Observed condensation time of dust grains in the nova ejecta, t_{cond} , versus nova speed class ($t_2[V]$, except for M31N 2007-07f, which is $t_2[R]$). Data for Galactic novae are given as open triangles, with the two suspected dust-forming novae in M31 shown as filled red squares. These, and the special cases of the Galactic novae PW Vul and V445 Pup, are discussed more fully in the text.

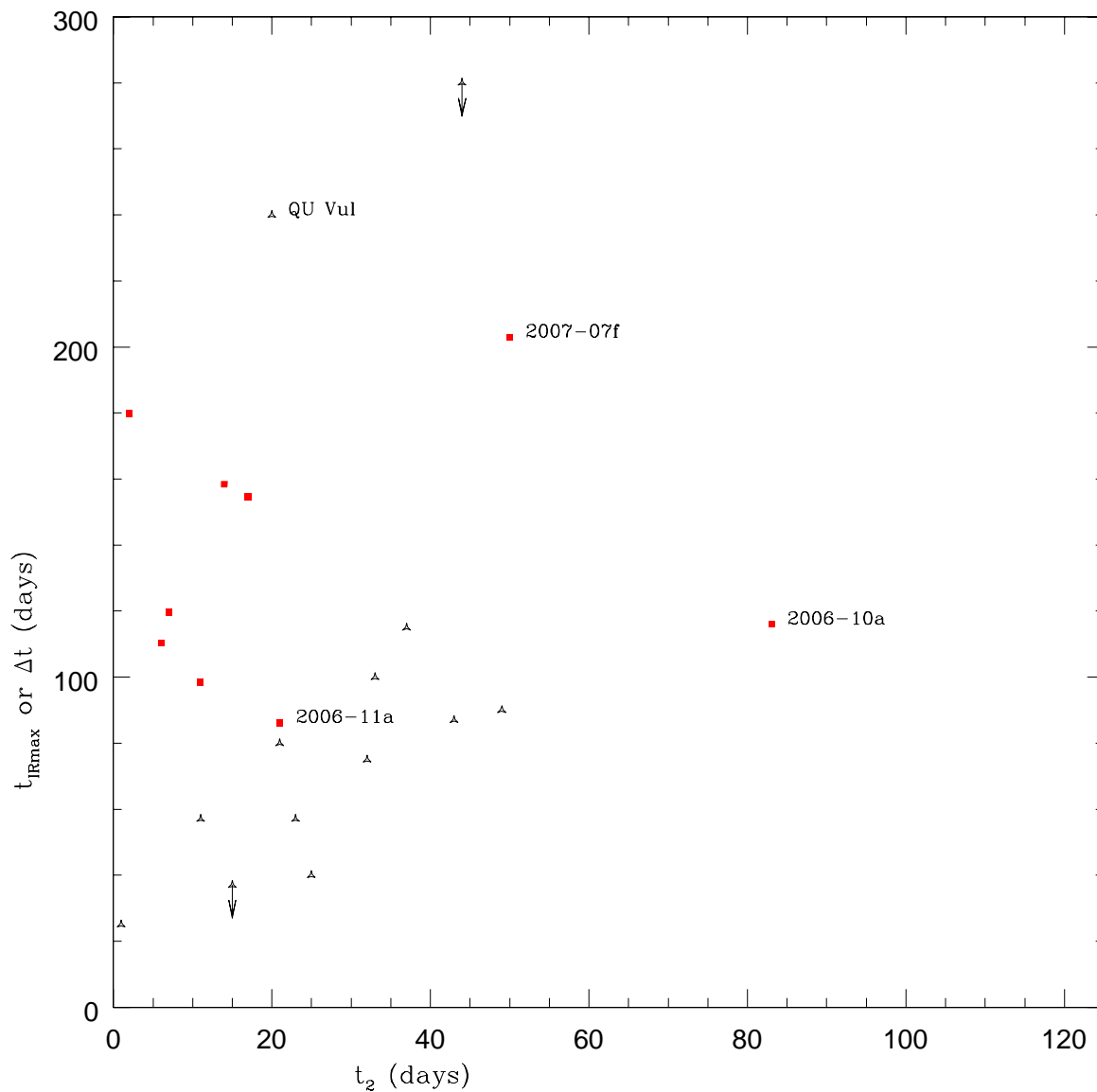


Fig. 12.— Time of infrared maximum, t_{IRmax} , versus nova speed class for Galactic novae (open triangles, t_{IRmax} data from Evans & Rawlings 2008, see also Table 11). An outlier is QU Vul, which is discussed more thoroughly in the text. Red squares denote the observations of novae in M31 Δt days after discovery (near optical maximum) with objects of particular interest noted (see text for details). Values of t_2 are from V -band measurements for M31N 2006-10a and the Galactic novae, while the M31 novae are mainly based on R -band measurements (again see text for details).

Table 1. Summary of *Spitzer* Observations

Nova	R.A.	Decl.	Discovery	<i>Spitzer</i>	Δt	Discovery
	(2000.0)	(2000.0)	HJD (2, 450, 000+)	HJD (2, 450, 000+)	(days)	Mag
IRAC						
M31N 2006-09c	00:42:42.38	+41:08:45.50	3996.64	4151.25	154.61	16.5(w)
M31N 2006-10a	00:41:43.23	+41:11:45.90	4034.31	4149.85	115.54	18.6(R)
M31N 2006-10b	00:39:27.46	+40:51:10.10	4039.59	4149.82	110.23	16.4(w)
M31N 2006-11a	00:42:56.61	+41:06:18.20	4064.97	4151.22	86.25	17.3(w)
M31N 2007-07f	00:38:42.20	+40:52:56.10	4292.48	4495.03	202.55	17.4(w)
M31N 2007-08a	00:40:54.40	+40:53:50.30	4318.80	4498.70	179.90	17.6(w)?
M31N 2007-08d	00:39:30.27	+40:29:14.20	4336.58	4495.06	158.48	18.1(R)
M31N 2007-10a	00:42:55.95	+41:03:22.00	4379.11	4498.73	119.62	16.3(R)?
IRS						
M31N 2006-09c	00:42:42.38	+41:08:45.50	3996.64	4142.04	145.40	16.5(w)
M31N 2006-10a	00:41:43.23	+41:11:45.90	4034.31	4141.99	107.68	18.6(R)
M31N 2006-10b	00:39:27.46	+40:51:10.10	4039.59	4142.08	102.49	16.4(w)
M31N 2006-11a	00:42:56.61	+41:06:18.20	4064.97	4141.95	76.98	17.3(w)
M31N 2007-08d	00:39:30.27	+40:29:14.20	4336.58	4519.34	182.76	18.1(R)
M31N 2007-10a	00:42:55.95	+41:03:22.00	4379.11	4519.30	140.19	16.3(R)?
M31N 2007-11d	00:44:54.90	+41:37:39.60	4421.02	4519.43	98.41	14.9(w)
M31N 2007-11e	00:45:47.74	+42:02:03.50	4432.58	4519.39	86.81	16.6(w)

Table 2. *Spitzer* IRAC Photometry

Nova	Flux (10^{-14} ergs cm^{-2} s^{-1} μm^{-1})			
	3.6 μm	4.5 μm	5.8 μm	8.0 μm
M31N 2006-09c	11.4 \pm 3.37	9.14 \pm 2.39	7.07 \pm 1.72	4.78 \pm 1.11
M31N 2006-10a	13.8 \pm 3.83	13.7 \pm 2.96	10.9 \pm 2.14	5.94 \pm 1.23
M31N 2006-10b	0.92 \pm 0.94	0.30 \pm 0.43	0.15 \pm 0.25	...
M31N 2006-11a	4.93 \pm 2.22	2.00 \pm 1.13	0.87 \pm 0.63	...
M31N 2007-07f	5.63 \pm 2.31	5.42 \pm 1.83	4.99 \pm 1.44	3.11 \pm 0.88
M31N 2007-08a
M31N 2007-08d	0.99 \pm 0.97	0.41 \pm 0.51	0.23 \pm 0.31	0.14 \pm 0.19
M31N 2007-10a

Table 3. Photometric Observations of M31N 2006-09c

HJD (2,450,000+)	Mag	Filter	Observer(s)	Telescope
3993.376	> 19.1	R	KH	Lelekovice 0.35-m
3996.404	18.1 ± 0.2	R	P. Kušnirák	Ondřejov 0.65-m
3999.609	17.15 ± 0.1	R	P. Kušnirák	Ondřejov 0.65-m
4000.317	17.0 ± 0.1	R	KH	Lelekovice 0.35-m
4000.590	17.35 ± 0.1	R	M. Wolf	Ondřejov 0.65-m
4001.360	17.3 ± 0.1	R	KH	Lelekovice 0.35-m
4002.302	17.4 ± 0.1	R	KH	Lelekovice 0.35-m
4002.329	17.5 ± 0.1	R	KH	Lelekovice 0.35-m
4005.312	17.8 ± 0.1	R	KH	Lelekovice 0.35-m
4007.312	17.9 ± 0.1	R	KH	Lelekovice 0.35-m
4014.295	19.0 ± 0.2	R	KH	Lelekovice 0.35-m
4017.258	19.1 ± 0.2	R	KH	Lelekovice 0.35-m
4019.319	18.8 ± 0.2	R	KH	Lelekovice 0.35-m
4024.383	19.3 ± 0.2	R	KH	Lelekovice 0.35-m
4026.330	19.3 ± 0.2	R	KH	Lelekovice 0.35-m
4026.364	19.3 ± 0.2	R	KH	Lelekovice 0.35-m
4034.312	19.9 ± 0.3	R	KH	Lelekovice 0.35-m
4256.677	$> 21.2 \pm 0.2$	B	MFB, MJD, AWS, KAM	LT 2.0-m
4260.700	$> 21.7 \pm 0.3$	B	MFB, MJD, AWS, KAM	LT 2.0-m
4260.705	$> 21.0 \pm 0.3$	V	MFB, MJD, AWS, KAM	LT 2.0-m
4260.690	$> 21.4 \pm 0.2$	r	MFB, MJD, AWS, KAM	LT 2.0-m
4260.695	21.8 ± 0.5	i	MFB, MJD, AWS, KAM	LT 2.0-m

Table 4. Photometric Observations of M31N 2006-10a

HJD (2, 450, 000+)	Mag	Filter	Observer(s)	Telescope
4019.319	> 19.7	R	KH	Lelekovice 0.35-m
4024.383	> 19.0	R	KH	Lelekovice 0.35-m
4026.330	> 20.1	R	KH	Lelekovice 0.35-m
4031.251	19.2 ± 0.25	R	KH	Lelekovice 0.35-m
4034.312	18.7 ± 0.15	R	KH	Lelekovice 0.35-m
4034.470	18.6 ± 0.15	R	P. Kušnirák	Ondřejov 0.65-m
4035.360	18.4 ± 0.3	R	KH	Lelekovice 0.35-m
4043.331	17.9 ± 0.1	R	KH	Lelekovice 0.35-m
4047.288	19.0 ± 0.3	R	KH	Lelekovice 0.35-m
4048.324	19.3 ± 0.2	R	KH	Lelekovice 0.35-m
4055.296	18.2 ± 0.15	R	KH	Lelekovice 0.35-m
4055.262	18.2 ± 0.1	R	P. Cagaš	Zlín 0.28-m
4070.308	19.2 ± 0.35	R	M. Wolf, P. Zasche	Ondřejov 0.65-m
4071.385	18.9 ± 0.2	R	P. Kušnirák	Ondřejov 0.65-m
4078.308	18.4 ± 0.3	R	KH	Lelekovice 0.35-m
4078.343	18.6 ± 0.2	R	KH	Lelekovice 0.35-m
4080.306	18.8 ± 0.25	R	KH	Lelekovice 0.35-m
4084.212	18.9 ± 0.2	R	KH	Lelekovice 0.35-m
4093.174	19.5:	R	KH	Lelekovice 0.35-m
4096.325	19.7 ± 0.25	R	KH	Lelekovice 0.35-m
4097.222	19.5 ± 0.25	R	KH	Lelekovice 0.35-m
4115.194	> 20.0	R	KH	Lelekovice 0.35-m
4121.381	> 19.8	R	KH	Lelekovice 0.35-m
4122.331	> 19.5	R	KH	Lelekovice 0.35-m
4122.377	> 19.4	R	KH	Lelekovice 0.35-m
4044.337	18.07 ± 0.04	B	MFB, MJD, AWS, KAM	LT 2.0-m
4050.589	19.06 ± 0.03	B	MFB, MJD, AWS, KAM	LT 2.0-m
4056.585	18.88 ± 0.03	B	MFB, MJD, AWS, KAM	LT 2.0-m
4062.606	18.58 ± 0.03	B	MFB, MJD, AWS, KAM	LT 2.0-m
4069.484	19.24 ± 0.04	B	MFB, MJD, AWS, KAM	LT 2.0-m
4071.549	19.06 ± 0.09	B	MFB, MJD, AWS, KAM	LT 2.0-m
4074.575	19.20 ± 0.11	B	MFB, MJD, AWS, KAM	LT 2.0-m
4077.542	19.26 ± 0.13	B	MFB, MJD, AWS, KAM	LT 2.0-m
4084.460	19.24 ± 0.03	B	MFB, MJD, AWS, KAM	LT 2.0-m
4092.454	19.93 ± 0.05	B	MFB, MJD, AWS, KAM	LT 2.0-m
4099.407	20.03 ± 0.11	B	MFB, MJD, AWS, KAM	LT 2.0-m
4101.393	19.78 ± 0.07	B	MFB, MJD, AWS, KAM	LT 2.0-m
4114.372	$> 21.90 \pm 0.24$	B	MFB, MJD, AWS, KAM	LT 2.0-m
4120.432	$> 20.89 \pm 0.28$	B	MFB, MJD, AWS, KAM	LT 2.0-m
4254.685	$> 17.6 \pm 0.9$	B	MFB, MJD, AWS, KAM	LT 2.0-m
4044.334	17.90 ± 0.03	V	MFB, MJD, AWS, KAM	LT 2.0-m
4050.586	19.10 ± 0.02	V	MFB, MJD, AWS, KAM	LT 2.0-m
4056.582	18.80 ± 0.03	V	MFB, MJD, AWS, KAM	LT 2.0-m

Table 4—Continued

HJD (2, 450, 000+)	Mag	Filter	Observer(s)	Telescope
4062.604	18.48 ± 0.02	V	MFB, MJD, AWS, KAM	LT 2.0-m
4069.481	19.25 ± 0.04	V	MFB, MJD, AWS, KAM	LT 2.0-m
4071.546	19.02 ± 0.12	V	MFB, MJD, AWS, KAM	LT 2.0-m
4074.572	19.39 ± 0.10	V	MFB, MJD, AWS, KAM	LT 2.0-m
4077.539	19.30 ± 0.05	V	MFB, MJD, AWS, KAM	LT 2.0-m
4084.457	19.16 ± 0.03	V	MFB, MJD, AWS, KAM	LT 2.0-m
4092.451	19.67 ± 0.05	V	MFB, MJD, AWS, KAM	LT 2.0-m
4099.404	19.64 ± 0.10	V	MFB, MJD, AWS, KAM	LT 2.0-m
4101.391	19.73 ± 0.06	V	MFB, MJD, AWS, KAM	LT 2.0-m
4114.370	$> 21.55 \pm 0.22$	V	MFB, MJD, AWS, KAM	LT 2.0-m
4120.429	$> 21.22 \pm 0.12$	V	MFB, MJD, AWS, KAM	LT 2.0-m
4254.692	$> 18.4 \pm 0.4$	V	MFB, MJD, AWS, KAM	LT 2.0-m
4254.671	$> 19.0 \pm 0.3$	r	MFB, MJD, AWS, KAM	LT 2.0-m

Table 5. Photometric Observations M31N 2006-10b

HJD (2,450,000+)	Mag	Filter	Observer(s)	Telescope
4043.888	18.95 ± 0.06	B	MFB, MJD, AWS, KAM	LT 2.0-m
4049.001	19.55 ± 0.04	B	MFB, MJD, AWS, KAM	LT 2.0-m
4057.034	20.39 ± 0.06	B	MFB, MJD, AWS, KAM	LT 2.0-m
4062.963	20.89 ± 0.07	B	MFB, MJD, AWS, KAM	LT 2.0-m
4068.945	20.99 ± 0.13	B	MFB, MJD, AWS, KAM	LT 2.0-m
4071.940	$> 20.14 \pm 0.21$	B	MFB, MJD, AWS, KAM	LT 2.0-m
4074.973	$> 20.35 \pm 0.20$	B	MFB, MJD, AWS, KAM	LT 2.0-m
4083.911	21.41 ± 0.10	B	MFB, MJD, AWS, KAM	LT 2.0-m
4098.938	$> 20.65 \pm 0.27$	B	MFB, MJD, AWS, KAM	LT 2.0-m
4105.915	$> 19.74 \pm 0.54$	B	MFB, MJD, AWS, KAM	LT 2.0-m
4113.883	$> 22.91 \pm 0.69$	B	MFB, MJD, AWS, KAM	LT 2.0-m
4119.958	$> 21.83 \pm 0.38$	B	MFB, MJD, AWS, KAM	LT 2.0-m
4248.204	$> 22.42 \pm 0.43$	B	MFB, MJD, AWS, KAM	LT 2.0-m
4048.998	20.02 ± 0.05	V	MFB, MJD, AWS, KAM	LT 2.0-m
4053.817	$> 17.33 \pm 0.29$	V	MFB, MJD, AWS, KAM	LT 2.0-m
4057.031	20.88 ± 0.07	V	MFB, MJD, AWS, KAM	LT 2.0-m
4062.960	21.27 ± 0.08	V	MFB, MJD, AWS, KAM	LT 2.0-m
4068.942	$> 21.69 \pm 0.23$	V	MFB, MJD, AWS, KAM	LT 2.0-m
4071.937	$> 20.12 \pm 0.21$	V	MFB, MJD, AWS, KAM	LT 2.0-m
4074.970	$> 20.64 \pm 0.19$	V	MFB, MJD, AWS, KAM	LT 2.0-m
4083.908	$> 22.30 \pm 0.22$	V	MFB, MJD, AWS, KAM	LT 2.0-m
4098.936	$> 20.51 \pm 0.22$	V	MFB, MJD, AWS, KAM	LT 2.0-m
4101.885	$> 20.13 \pm 0.33$	V	MFB, MJD, AWS, KAM	LT 2.0-m
4105.912	$> 17.61 \pm 0.60$	V	MFB, MJD, AWS, KAM	LT 2.0-m
4107.986	$> 18.40 \pm 0.28$	V	MFB, MJD, AWS, KAM	LT 2.0-m
4113.880	$> 21.96 \pm 0.39$	V	MFB, MJD, AWS, KAM	LT 2.0-m
4119.955	$> 22.76 \pm 0.65$	V	MFB, MJD, AWS, KAM	LT 2.0-m
4248.209	$> 22.30 \pm 0.43$	V	MFB, MJD, AWS, KAM	LT 2.0-m
4248.193	$> 22.9 \pm 0.4$	r	MFB, MJD, AWS, KAM	LT 2.0-m
4248.199	$> 21.5 \pm 0.3$	i	MFB, MJD, AWS, KAM	LT 2.0-m

Table 6. Photometric Observations M31N 2006-11a

HJD (2, 450, 000+)	Mag	Filter	Observer(s)	Telescope
4048.324	> 19.8	R	KH	Lelekovice 0.35-m
4055.296	> 19.8	R	KH	Lelekovice 0.35-m
4070.263	16.9 ± 0.1	R	M. Wolf, P. Zasche	Ondřejov 0.65-m
4070.308	16.6 ± 0.15	R	M. Wolf, P. Zasche	Ondřejov 0.65-m
4078.308	16.1 ± 0.1	R	KH	Lelekovice 0.35-m
4078.343	16.0 ± 0.1	R	KH	Lelekovice 0.35-m
4080.306	16.3 ± 0.1	R	KH	Lelekovice 0.35-m
4084.212	16.9 ± 0.1	R	KH	Lelekovice 0.35-m
4093.174	17.7 ± 0.15	R	KH	Lelekovice 0.35-m
4096.325	17.8 ± 0.15	R	KH	Lelekovice 0.35-m
4097.222	17.8 ± 0.15	R	KH	Lelekovice 0.35-m
4115.194	18.8 ± 0.2	R	KH	Lelekovice 0.35-m
4121.381	18.9 ± 0.2	R	KH	Lelekovice 0.35-m
4122.331	19.2 ± 0.25	R	KH	Lelekovice 0.35-m
4122.377	19.1 ± 0.3	R	KH	Lelekovice 0.35-m
4126.289	19.3 ± 0.3	R	KH	Lelekovice 0.35-m
4126.339	19.1 ± 0.3	R	KH	Lelekovice 0.35-m
4128.275	19.2 ± 0.25	R	KH	Lelekovice 0.35-m
4135.298	19.4 ± 0.3	R	KH	Lelekovice 0.35-m
4135.334	19.3 ± 0.25	R	KH	Lelekovice 0.35-m
4141.362	19.2 ± 0.3	R	KH	Lelekovice 0.35-m
4146.295	19.4 ± 0.25	R	KH	Lelekovice 0.35-m
4149.273	19.4 ± 0.25	R	KH	Lelekovice 0.35-m
4166.247	19.7 ± 0.2	R	KH	Ondřejov 0.65-m
4167.366	20.0 ± 0.35	R	KH	Ondřejov 0.65-m
4170.264	20.0 ± 0.3	R	KH	Ondřejov 0.65-m
4173.269	19.8 ± 0.25	R	P. Kušnirák, T. Henych	Ondřejov 0.65-m
4174.268	> 19.7	R	KH	Lelekovice 0.35-m
4240.561	> 20.0	R	KH	Ondřejov 0.65-m
4140.868	20.12 ± 0.05	B	MFB, MJD, AWS, KAM	LT 2.0-m
4140.872	20.54 ± 0.06	V	MFB, MJD, AWS, KAM	LT 2.0-m
4140.856	19.22 ± 0.03	r	MFB, MJD, AWS, KAM	LT 2.0-m
4140.862	20.22 ± 0.08	i	MFB, MJD, AWS, KAM	LT 2.0-m

Table 7. Photometric Observations of M31N 2007-08d

HJD (2, 450, 000+)	Mag	Filter	Observer(s)	Telescope
4380.401	18.6 ± 0.2	R	KH, P. Kušnirák	Ondřejov 0.65-m
4380.424	18.5 ± 0.15	R	KH, P. Kušnirák	Ondřejov 0.65-m
4382.235	19.0 ± 0.25	R	KH, P. Kušnirák	Ondřejov 0.65-m
4387.219	> 19.5	R	KH, P. Kušnirák	Ondřejov 0.65-m
4387.231	19.5 ± 0.3	R	KH, P. Kušnirák	Ondřejov 0.65-m
4387.561	19.6 ± 0.2	R	KH	Ondřejov 0.65-m
4388.227	19.8 ± 0.25	R	KH, P. Kušnirák	Ondřejov 0.65-m
4388.626	19.6 ± 0.35	R	KH	Ondřejov 0.65-m
4389.233	19.8 ± 0.3	R	KH, P. Kušnirák	Ondřejov 0.65-m
4389.646	20.0 ± 0.3	R	KH	Ondřejov 0.65-m

Table 8. Summary of HET Spectroscopic Observations

Nova	R.A. (2000.0)	Decl. (2000.0)	UT Date	Exp. (sec)	Coverage (Å)	Weather
M31N 2006-09c	00 42 42.38	41 08 45.5	24.18 Sep 2006	1800	4275–7250	Spec
M31N 2006-10a	00 41 43.23	41 11 45.9	30.31 Oct 2006	1500	4275–7250	Spec
M31N 2006-10b	00 39 27.38	40 51 09.8	23.24 Nov 2006	1200	4275–7250	Phot
M31N 2006-11a	00 42 56.81	41 06 18.4	28.23 Nov 2006	1200	4275–7250	Spec
M31N 2007-08d	00 39 30.27	40 29 14.2	13.44 Sep 2007	1200	4275–7250	Spec
M31N 2007-10a	00 42 55.95	41 03 22.0	19.13 Oct 2007	1400	4275–7250	Phot
M31N 2007-11d	00 44 54.60	41 37 40.0	04.22 Dec 2007	1200	4100–8900	Phot
M31N 2007-11e	00 45 47.74	42 02 03.5	05.23 Dec 2007	1200	4100–8900	Phot

Table 9. Balmer Emission Line Properties

Nova	EW (Å)		FWHM (km/s)	
	H β	H α	H β	H α
M31N 2006-09c	–127	–470	1910	1920
M31N 2006-10a	–44	–90	950	810
M31N 2006-10b	–133	–2130	3030	3562
M31N 2006-11a	–35	–57	1420	1120
M31N 2007-07f ^a	–56	–195	1340	1110
M31N 2007-08a	...	–66	...	1880
M31N 2007-08d	–68	–284	1160	1180
M31N 2007-10a	–37	–154	470	500
M31N 2007-11d	–297	–1223	2060	2260
M31N 2007-11e	–137	–306	1750	1600

^aMeasurements are from a spectrum kindly provided by R. Quimby (private communication).

Table 10. Spatial Positions and Spectroscopic Types

Nova	$\Delta\alpha \cos\delta$ (')	$\Delta\delta$ (')	a (')	Type	References ^a
M31N 2006-09c	−0.37	−7.39	11.61	Fe II	1,2
M31N 2006-10a	−11.50	−4.36	17.31	Fe II	1
M31N 2006-10b	−37.25	−24.81	63.14	He/N	1
M31N 2006-11a	2.35	−9.84	20.46	Fe II	1
M31N 2007-07f	−45.77	−22.95	81.74	Fe II	3
M31N 2007-08a	−20.78	−22.25	30.49	Fe II? ^b	4
M31N 2007-08d	−36.91	−46.74	59.56	Fe II	1
M31N 2007-10a	2.19	−12.78	27.57	Fe II? ^c	1, 5
M31N 2007-11d	24.34	21.60	34.03	Fe II	1, 6, 7
M31N 2007-11e ^d	34.06	46.07	57.52	Fe II	1, 8

^aReferences: (1) This work; (2) Shafter et al. (2006); (3) Quimby (2007); (4) Barsukova et al. (2007); (5) Gal-Yam & Quimby (2007); (6) Quimby et al. (2007); (7) Shafter et al. (2009); (8) Di Mille et al. (2007)

^bpossible Hybrid nova

^cpossible peculiar He/N nova with narrow He I lines

^dNeon nova

Table 11. Eruption Properties and Dust Formation Timescales

Nova	t_2^a (days)	t_{cond} (days)	t_{IRmax} (days)	ΔT (days)	Type
V1370 Aql	15	< 16	37	...	He/N
V1419 Aql	25	~90	40	...	Fe II
OS And	11	22	Fe II
T Aur	80	87	Fe II
V705 Cas	33	63	100	...	Fe II
V842 Cen	43	36	87	...	Fe II
V476 Cyg	7	40	Fe II
V1668 Cyg	11	33	57	...	Fe II
V2274 Cyg	22	40	Fe II
DQ Her	76	105	Fe II
V827 Her	21	43
V838 Her	1.2	18	25	...	He/N
V445 Pup	215	218
V732 Sgr	65	73
FH Ser	49	60	90	...	Fe II
LW Ser	32	23	75	...	Fe II
V992 Sco	100	93	Fe II
NQ Vul	21	62	80	...	Fe II
PW Vul	44	154	280	...	Fe II
QU Vul	20	40	240	...	Fe II
QV Vul	37	56	115	...	Fe II
LMC 1998#1	23	59	57
M31N 2006-09c	17(<i>R</i>)	154.61	Fe II
M31N 2006-10a	74(<i>B</i>), 83(<i>V</i>), 112(<i>R</i>)	< 116	...	116	Fe II
M31N 2006-10b	20(<i>B</i>), 6(<i>R</i>)	110.23	He/N
M31N 2006-11a	21(<i>R</i>)	86.25	Fe II
M31N 2007-07f	50 : (<i>R</i>)	< 203	...	203	Fe II
M31N 2007-08a	2	158.48	Fe II?
M31N 2007-08d	14(<i>R</i>)	179.9	Fe II
M31N 2007-10a	7	119.62	Fe II?
M31N 2007-11d	14(<i>B</i>), 11(<i>V</i>), 10(<i>R</i>)	98.37	Fe II
M31N 2007-11e	27 : (<i>R</i>)	86.8	Fe II

^aGalactic nova t_2 times from Strope et al. (2010)